Optimal Control in Energy Conversion of Small Wind Power Systems with Permanent-magnet-synchronous-generators

C. VLAD, I. MUNTEANU, A.I. BRATCU, E. CEANGĂ
"Dunărea de Jos" University of Galați
47, Domnească, 800008-Galați
ROMANIA
{ciprian.vlad, iulian.munteanu, antoneta.bratcu, emil.ceanga}@ugal.ro

Abstract: - This paper presents the results of experimental investigation of a low-power wind energy conversion system (WECS), based on a permanent-magnet synchronous generator (PMSG) connected directly to the turbine. A development system was built in order to carry out the experiments. Its detailed description is also provided. The development system can work as an autonomous system for remote sites or as a grid-connected system, illustrating the concept of distributed production of electrical energy. It includes a wind turbine simulator, which is speed or torque controlled and offers a "wind shaft", where the static and dynamic characteristics of a turbine are obtained. The wind shaft generator drives a permanent magnet synchronous generator (PMSG). The other components of the hybrid system are: a battery, a classical source and, possibly, a PV source. The hardware/software application is based on the dSPACE system. The experimental results show that the performance of a multi-polar-PMSG-based small wind power system is strongly determined by the generator's behaviour. Two optimal regimes characteristics (ORC) are defined in this paper: the first one represents the mechanical power versus the rotational speed (ORC_m) and the second one is the electrical power delivered to a load versus the rotational speed (ORC_e). An optimal control loop aiming to maximize the delivered electrical power is designed, namely its reference is computed based on the ORC_e. In this way, the global efficiency of the energy conversion is maximized. The effectiveness of the proposed optimal control loop is illustrated by experimental results.

Key-Words: - wind system, optimal control, permanent-magnet synchronous generator, hardware-in-the-loop simulation, maximum power point tracking.

1 Introduction

The problem of renewable energy conversion and, in particular, the conversion of wind energy is highly topical and raises many specific tasks for scientific research [1]. For basic aspects concerning wind power systems, there is a very broad-based literature [2], most of which deals with the optimal control of wind energy conversion [3]-[5]. Generally, there are studies dedicated to high-power wind energy systems, using simulation tools [6], [7]. Compared to high-power wind energy systems, the low-power plants can be studied experimentally in laboratory. In this case, the research objectives may be various: optimizing the conversion of wind energy [8]–[13], operation in stand-alone regime [14]–[17], design of hybrid systems [18], integrated systems for distributed production of electrical energy using renewable energy sources, *etc*.

Nowadays, multi-polar permanent-magnet synchronous generators (PMSG) represent an important solution to the design of wind energy conversion systems (WECS), offering some advantages versus the asynchronous generators, *e.g.*, a simpler mechanical structure. The maximum power point tracking control of such systems is analyzed in [2]-[4]. WECS optimization with an energy criterion is dealt with especially for high-power WECS. In the case of low-power WECS, PMSG are widely used because they allow that the generator be coupled directly to the wind turbine shaft. The optimal control of these systems is treated in two distinct situations. The first is when the WECS delivers power to a battery, by means of a charge regulator [5], [9] and [10]. This regulator imposes operation constraints which do not allow rigorous tracking of the optimal regimes characteristic (ORC). In the second situation the WECS operates on the ORC, but in [11]-[14] only numerical simulation results are reported.

Detailed analysis of PMSG, including experiments, has lead to the necessity of taking into account the features of this kind of generator in its various applications. In [15] one can find experimental results illustrating the behaviour of a

medium-power PMSG (S_n = 125 kVA). For lower power (*e.g.*, S_n = 2.5 kVA in [15]), the issue of considering the influence of PMSG characteristics on the autonomous WECS becomes even more important.

In this paper are presented experimental results concerning the properties of a low-power PMSG-based WECS with direct coupling between the generator and the turbine shaft. A development system was built in order to carry out the experiments; its detailed description is also provided. The development system is based on low-power PMSG-based wind energy conversion systems (WECS) with direct coupling between the generator and the turbine shaft.

Two optimal regimes characteristics (ORC) of the wind system are defined: the first one represents the mechanical power versus the rotational speed (ORC_m) and the second one is the electrical power delivered to a load versus the rotational speed (ORC_e). For the low-power PMSG-based wind energy systems, the ORC_e is not obtained from ORC_m by a simple sub unitary coefficient (PMSG's efficiency). Instead of maximizing the aerodynamic efficiency, as in most of the works in the literature, a new optimal regimes characteristic is defined, which passes through points of ORC_e. Experimental results are discussed, that suggest the effectiveness of the approach.

The rest of the paper is organized as follows. The next section describes the experimental rig used to carry out the real-time tests. The third section presents the WECS steady-state characteristics, whereas the fourth section discusses the main results of maximum power point tracking control. The last section is dedicated to conclusions.

2 Experimental Rig

The experimental rig was built as a development system that aims at experimentally researching low-power hybrid renewable energy systems used for distributed production. It is composed of two subsystems:

1) The electromechanical subsystem;

2) The electrical, control and supervision subsystem.

The hardware/software support of the whole experimental rig is ensured by the dSPACE board DS 1103.

The basic elements of the development system are shown in Fig. 1. Here are specified: wind turbine (in the experimental rig, an elctromechanical wind turbine simulator is utilized); electrical generator (PMSG), diesel-generator, battery; PV source, choppers; inverter; D.C. link: A.C. link etc.

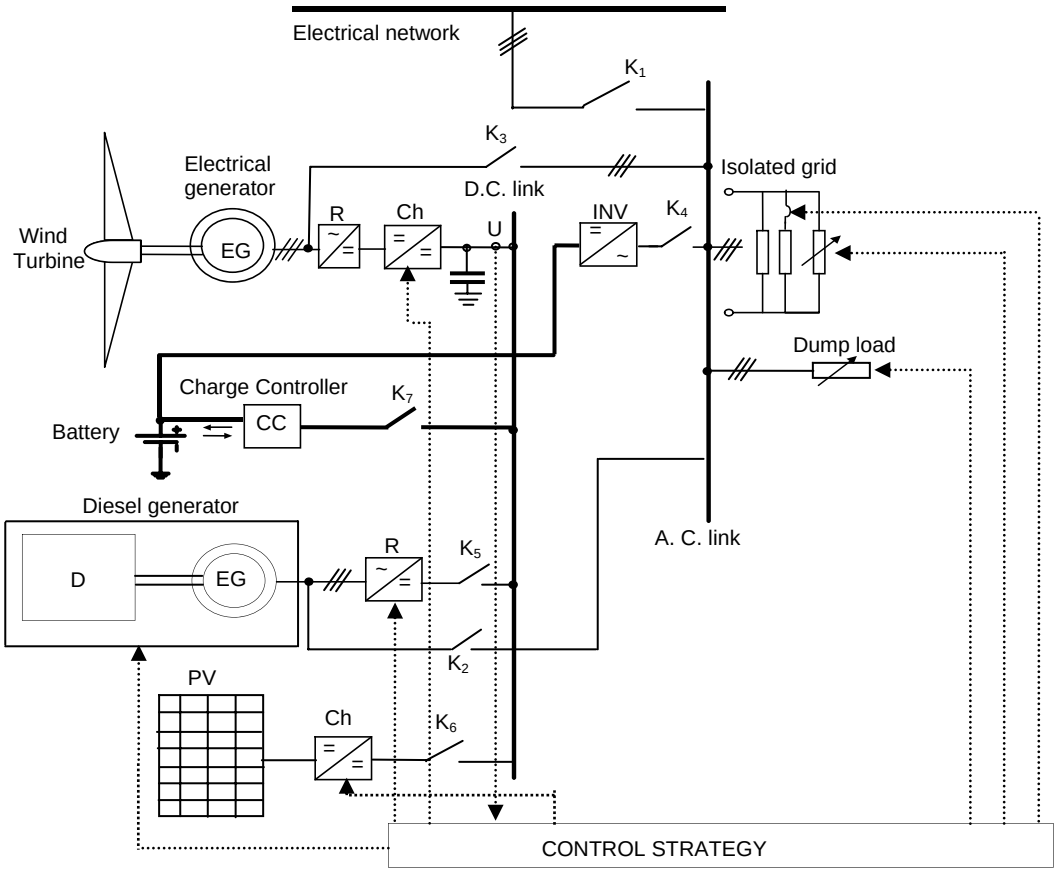

Fig.1. Development systems' structure

The electromechanical wind turbine simulator is built based upon the hardware-in-the-loop simulation concept [3]. This simulator provides a "wind shaft" where the steady-state and dynamic characteristics of a given turbine can be replicated. The simulator is composed of:

- A closed-loop servo-system, consisting of a Danfoss VLT 5005 Flux inverter, which controls an asynchronous motor with 960 rpm rated speed and 3 kW rated power. This means that wind turbines of 3 kW maximum rated power can be simulated;

- A real-time software simulator (RTSS), implementing the turbine dynamic model and the wind speed model [17]-[20].

In Fig.2 the principle of wind turbine simulator is illustrate.

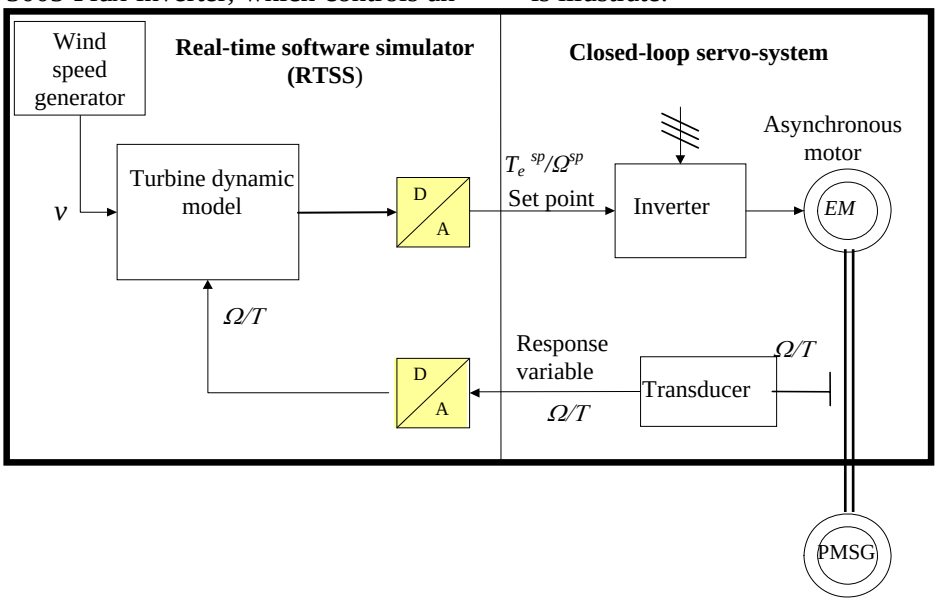

Fig.2. Wind turbine simulator: principle

The servo-system can be controlled by the RTSS in two ways:

- By means of a speed control loop: the RTSS imposes a speed reference to the servo-system and this one responds by sending back the estimated electromagnetic torque of the asynchronous motor as "*response variable*";

- By means of a torque control loop, when the servo-system receives a torque reference and responds by sending back to the RTSS the measured shaft rotational speed.

The results presented in the following have been obtained by controlling the speed of the simulator. This solution has been chosen as it is less affected by noise.

The wind turbine shaft is directly coupled to a Southwest Windpower® Whisper WHI 200 PMSG, having 1 kW rated power. The power limitation of this turbine is ensured by stall control.

The most important wind turbine characteristic implemented in the RTSS is that of the torque coefficient, $C_T(\lambda)$, where λ is the tip speed ratio of the considered wind turbine. Three situations can be encountered when choosing this characteristic:

a – $C_T(\lambda)$ is considered known (given);

b – a generic $C_T(\lambda)$ curve is adopted, which is parameterised such that the optimal tip speed, λ_{opt}, to be adjusted within narrow limits (λ_{opt}, = 6...8), without modifying the general form of the curve (Fig.3);

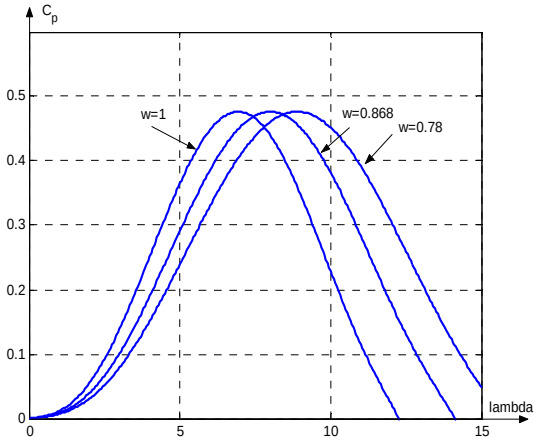

Fig.3. Parameterized characteristics of the wind turbine

c – $C_T(\lambda)$ is obtained starting from the constructive dimensions of the simulated wind turbine. In this case, the constructive features of blades (chord variation along the blade, pitch angle variation, number of blades, *etc.*) are established in a preliminary stage, then a software program is used

to generate the $C_T(\lambda)$ curve based upon the blade element method [16].

An important function of the RTSS is the real-time wind speed generation. The subsystem achieving this function can ensure three distinct regimes:

a – constant speed regime, adjustable in real time through the ControlDesk® interface accompanying the dSPACE board;

b – turbulent wind regime, where the average wind speed is adjustable in real time through the ControlDesk® interface. The wind speed turbulence component depends of the current average wind speed and is obtained with a second-order rational shaping filter by imposing a desired value of the turbulence intensity, I_t:

$$I_t = \sigma_t / \overline{v} \quad (1)$$

where σ_t is the standard deviation of the turbulence component and $\overline{v}$ is the average wind speed. The turbulence intensity is established upon von Karman's or Kaimal's expressions of the spectral density function by using computation relations according to some usual standards: IEC 1400-1, Danish standard DS 472, *etc*. These relations have as parameters the ground surface roughness and the height from the ground [21], [22]. The transfer function of the rational shaping filter using von Karman's model of turbulence is:

$$H_t(s) = K_F \cdot \frac{m_1 T_F s + 1}{(T_F s + 1)(m_2 T_F s + 1)} \quad (2)$$

where $m_1 = 0.4,\ m_2 = 0.25$ and turbulence parameters K_F and T_F are computed in function of the average wind speed [22], [23].

The experimental rig's structure has a load adaptation circuit in order to ensure operation of the turbine on the ORC_e regime. The load adaptation circuit, coupled at the PMSG output, is composed of a rectifier and a chopper embedded in the power optimal control loop (Fig.4).

The sampling time of the real-time application is 0.2 ms.

The general aspect of the experimental rig is presented in the Appendix.

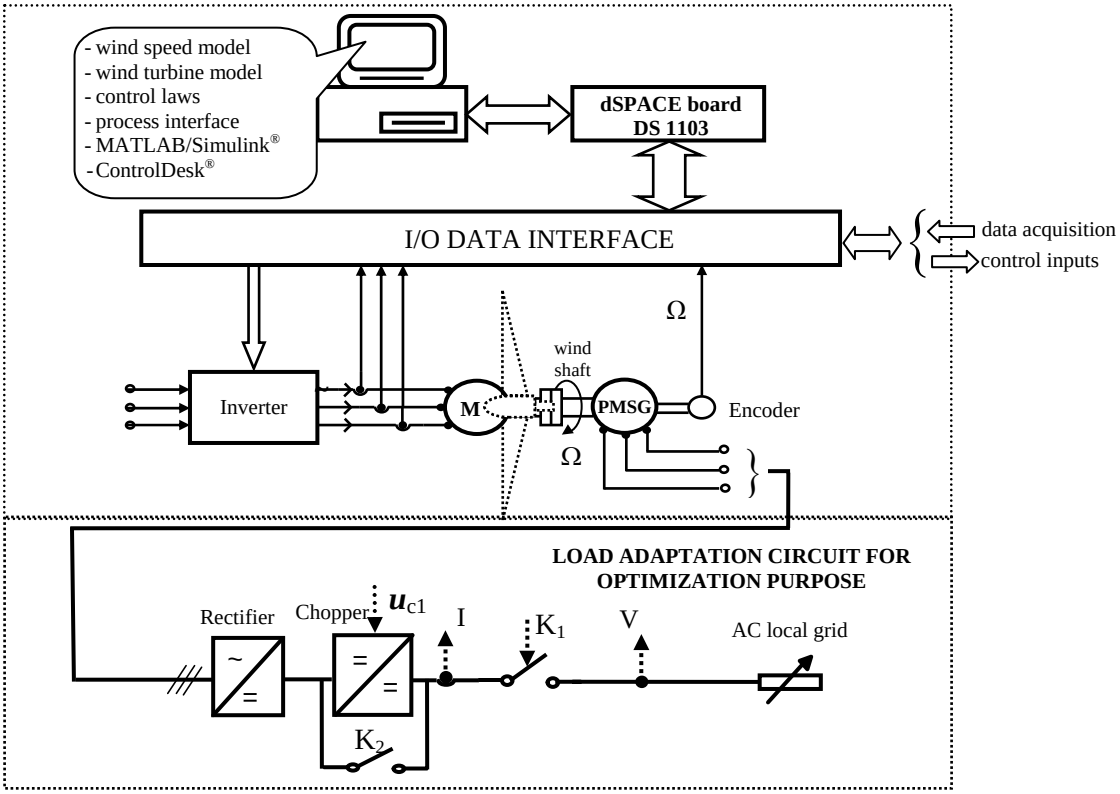

Fig.4. Block diagram of the experimental rig in the optimization regime

3 Experimental steady-state characteristics of WECS

The rig monitoring is possible due to the ControlDesk® interface of the dSPACE system. The main functions are performed:

- Time evolutions of measured variables (currents, voltages, angular speed, electromagnetic torque) and of computed values (tip speed ratio, power coefficient, wind speed etc.);
- Excursion of the operating point in the torque-speed plane;
- Real-time choice of the wind regime and of the

average wind speed;
- Selection of the tracking control loop operation mode for wind turbine optimization ("open - MAN" or "closed - AUT") and the choice of the controller parameters, etc.

Using the monitoring system, the steady-state characteristics of WECS have been determined when the PMSG delivers power to the load resistance through the rectifier (switches K_1 and K_2 turned on in Fig.4). In Fig.5 we can see the following curves:

a – mechanical power versus rotational speed, Ω, and wind speed, v – this curve is denoted by $P_m(\Omega,v)$ and drawn with dashed line;

b – electrical power, denoted by $P_e(\Omega,v)$, drawn with solid line.

The circles in graphs from Fig.5 denote the points obtained experimentally. One can note sensible differences between the two curve families. This situation poses specific problems in optimization strategies.

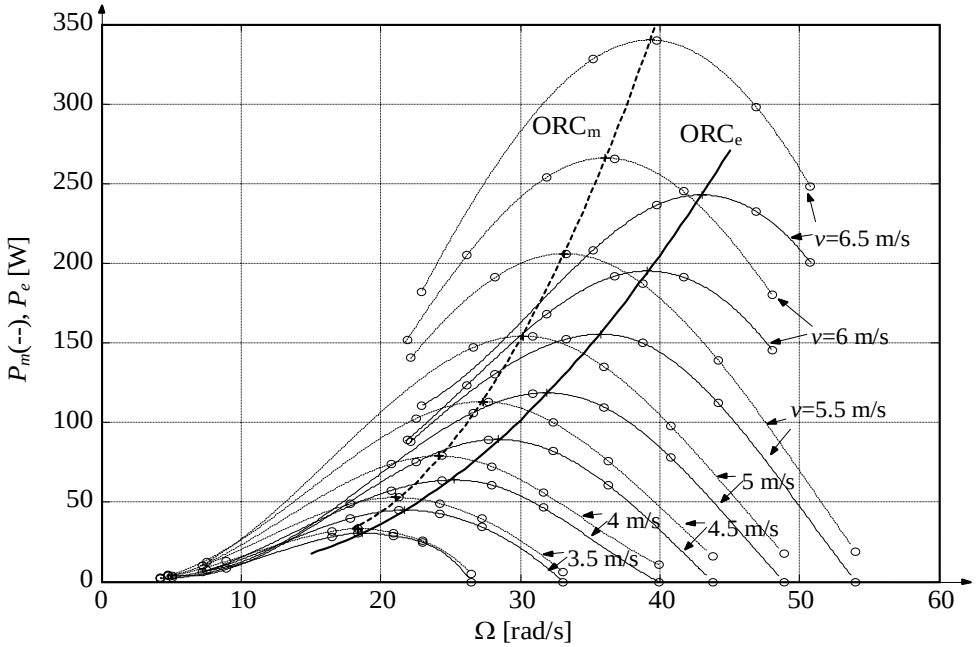

Fig.5. Experimental curves $P_m(\Omega,v)$ (dashed) and $P_e(\Omega,v)$ (solid)

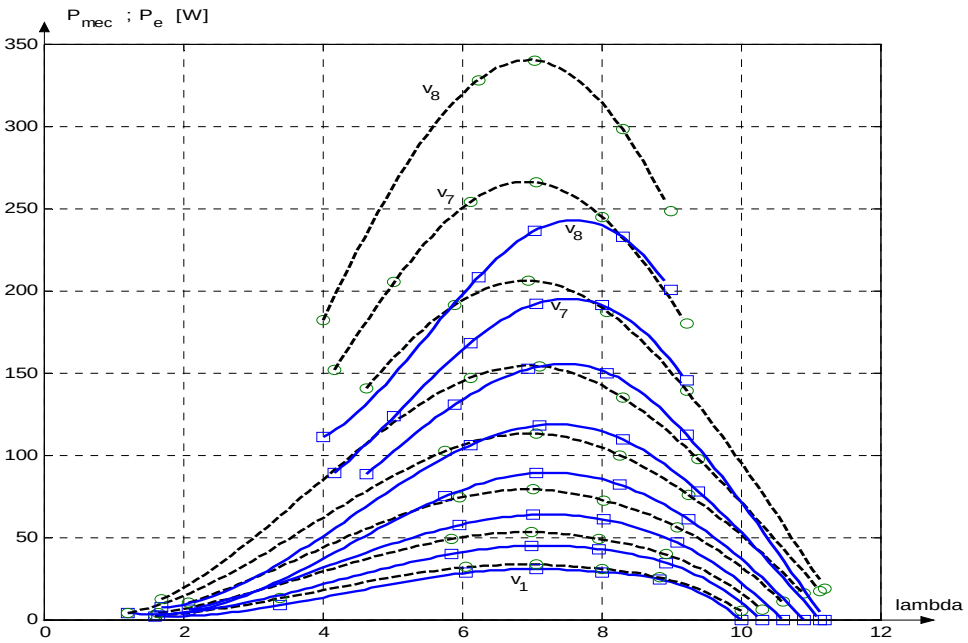

Fig.6. Experimental curves $P_m(\lambda)$ (dashed) and $P_e(\lambda)$ (solid)

As expected, values of electrical power, P_e, are below the corresponding values of mechanical power, P_m, because of the low efficiency of low-power multi-polar PMSG. But an unexpected result is that the $P_e(\Omega,v)$ curves are drifted to the right in relation to the $P_m(\Omega,v)$ curves. Therefore, there are in fact two optimal regimes characteristics that can be defined when the wind speed varies, namely:
- ORC_m, *i.e.*, the locus of maximum *mechanical* power points;
- ORC_e, *i.e.*, the locus of points of maximum *electrical* power delivered to the load.

When formulating the WECS optimal control problem the interest is obviously focused on the ORC_e. This problem requires a control solution that is modified in relation to that employed for high-power WECS.

The experimental characteristics $P_m(\lambda)$ have the maximum at λ=7, but the maxima of characteristics $P_e(\lambda)$ are not obtained for a constant value of the tip speed ratio (Fig.6). So, for optimizing the wind system within electrical power can't use any more the conservation tip speed ratio principle ($\lambda = \lambda_{\text{opt}}$).

4 Results concerning the Maximum Power Point Tracking Control

The aerodynamic power is:

$$P_{wind} = \frac{1}{2} \cdot C_p \cdot \rho \cdot A_r \cdot v^2 \tag{3}$$

where $C_p(\lambda)$ – power efficiency coefficient of the turbine; ρ - air density [kg/m^3]; A_r – rotor swept area [m^2]; v – single point wind speed in the axial direction [m/s]; λ – tip speed ratio:

$$\lambda = \frac{\Omega_t \cdot R}{v} \tag{4}$$

with Ω_t and R - rotational speed of wind turbine and blade length, respectively. The mechanical rotor torque (T_{wind}) is given by:

$$T_{wind} = \frac{P_{wind}}{\Omega_t} = \frac{1}{2} \cdot C_p \cdot \rho \cdot A_r \cdot \frac{v^3}{\Omega_t} \tag{5}$$

The permanent-magnet synchronous generator (PMSG) is direct connected to the turbine shaft, there is no drive train.

In the case of high-power WECS, the optimization control loop is achieved by tracking an optimal power reference, which in turn depends on the maximum mechanical power that is [20]:

$$P_{opt}^r = K \cdot \Omega^3 \tag{6}$$

with:

$$K = 0.5 \cdot C_P(\lambda_{opt}) \cdot \rho \pi R^5 / \lambda_{opt}^3 \tag{7}$$

where λ_{opt} is the optimal tip speed ratio. It is considered that the mechanical to electrical energy conversion efficiency is close to 1, whereas the theoretical efficiency of the wind to mechanical energy conversion is given by the Betz limit, $C_{P\max} = 0.59$ [21].

Unlike the high-power WECS (including those with PMSG), the low-power multi-polar PMSG-based WECS have quite reduced mechanical to electrical conversion efficiency. Hence, the ORC_e differs from the ORC_m in a non-negligible degree.

In order to obtain the reference of the electrical power loop, the ORC_e given in Fig.5 has been parameterised by polynomial regression. Thus, the optimal electrical power that has been imposed to the tracking loop is:

$$P_{e,opt}^r = 0.0081356\Omega^3 - 0.555\Omega^2 + 18.6\Omega - 179.1 \tag{8}$$

The experimental results illustrating the optimal operation of WECS can be seen in the ControlDesk® captures shown in Fig.7 and 8. In Fig.7 one can see how the optimized WECS evolves in a pseudo-steady-state regime ensured by a slow ramp variation of the wind speed. One can see that, once the starting regime was finished, the optimal tip speed slightly differs from its optimal value that corresponds to the wind to mechanical energy conversion (in this case, $\lambda_{opt} = 7$).

Among the variables displayed in Fig.7 one can see the error of the optimal power tracking loop. In the $C_T - \Omega$ plane the wind torque – rotational speed curve is obtained for the initial value of the wind speed, v=4 m/s, during the starting regime, then the ORC_e is obtained as the wind speed increases slowly with constant gradient.

Fig.8 illustrates the operation of the optimized WECS as the wind speed varies stochastically. One can see how the optimal operating point evolves around the ORC_e. Moreover, the dynamical errors of tracking the power reference (8) are small versus the reference value.

Similar results have been obtained for system optimization within mechanical power.

For a thoroughly comparative analysis of the wind system optimal regimes, within electrical and mechanical power, two variables (tip speed ratio, $\lambda(t)$, and power coefficient, $C_P(t)$, were distinctly

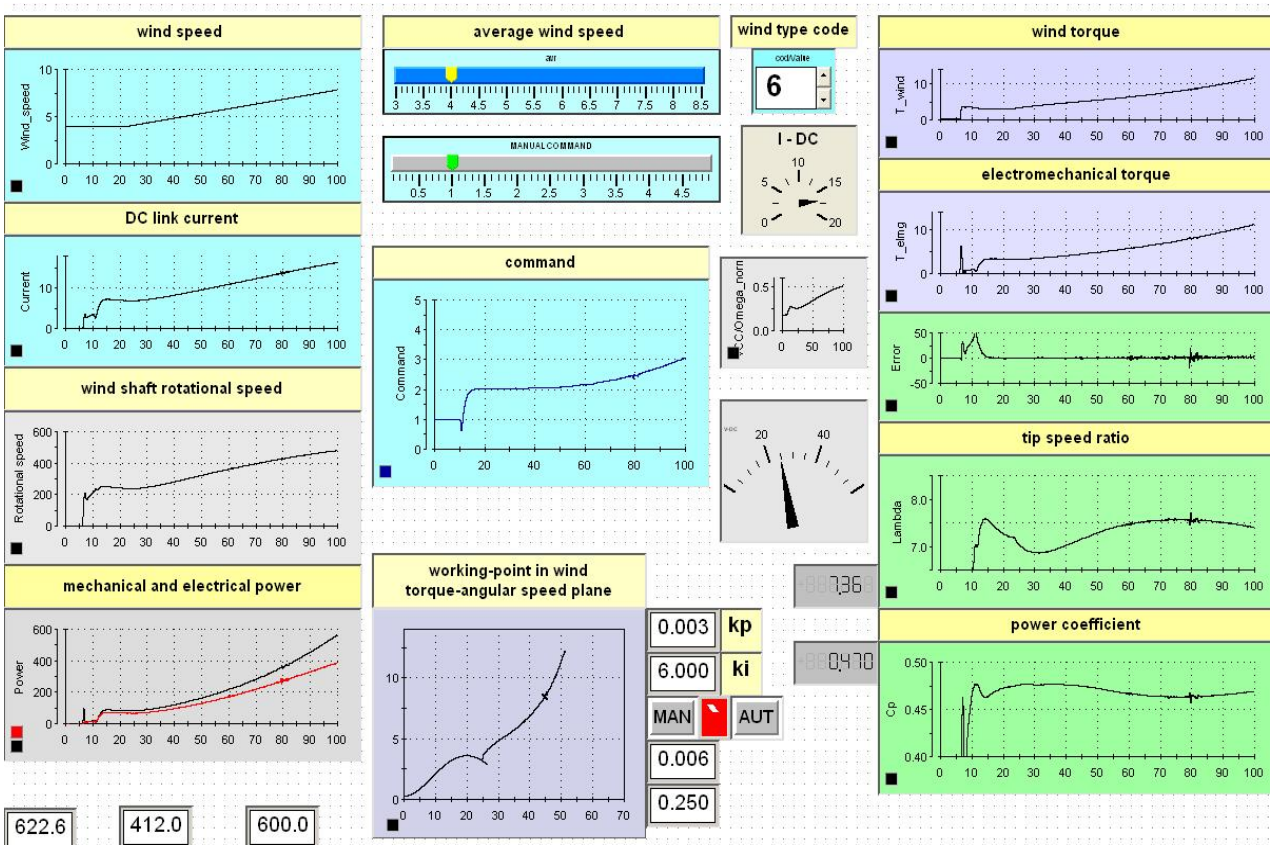

Fig.7. Response of the optimized WECS to a ramp change in the wind speed

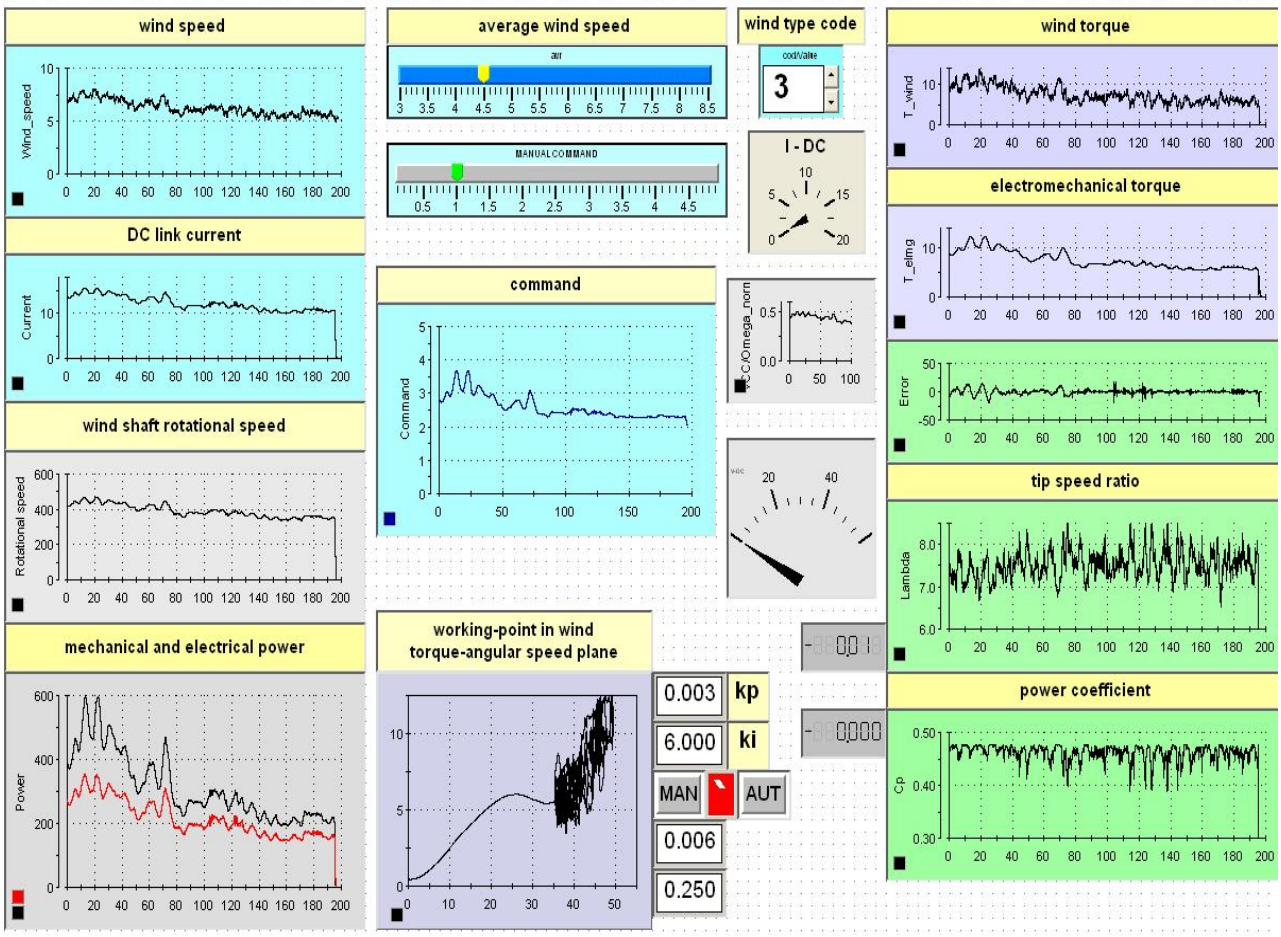

Fig.8. Response of the optimized WECS to a stochastic wind speed sequence

analyzed). In Fig.9 one can see tip speed variations for a wind speed increasing slowly with constant gradient starting from 4 m/s. The curve from Fig.9.b is taking over straight from Fig.7 screen and has been obtain from the optimization regime within electrical power.

Fig.9.a belongs to optimization regime within mechanical power. After the starting regime, one can see very small dynamical errors of the optimization loop and that $\lambda(t) \cong \lambda_{opt} = 7$.

When optimizing within electrical power, the tip speed ratio is variable, having a different value from the optimal mechanical regime. ($\lambda_{opt} = 7$).

Similar results are obtained when the wind speed varies stochastically. For the mechanical power within optimization regime the tip speed ratio evolves around $\lambda_{opt} = 7$ (Fig.10.a) and for the electrical power's one the mean tip speed ratio value varies around 7.5 (Fig.10.b).

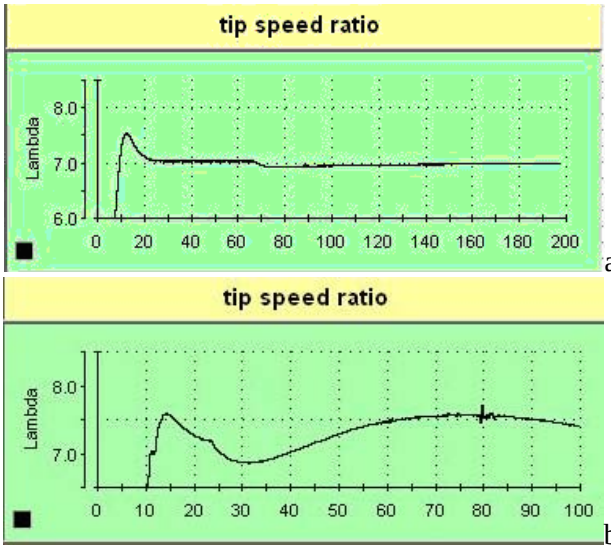

Fig.9.

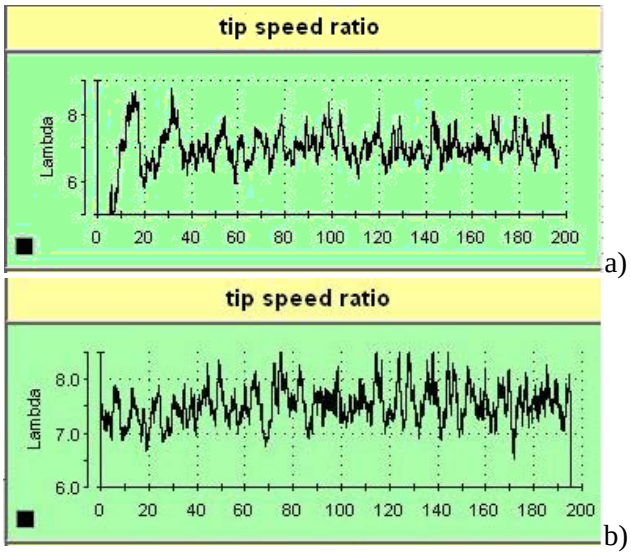

Fig.10.

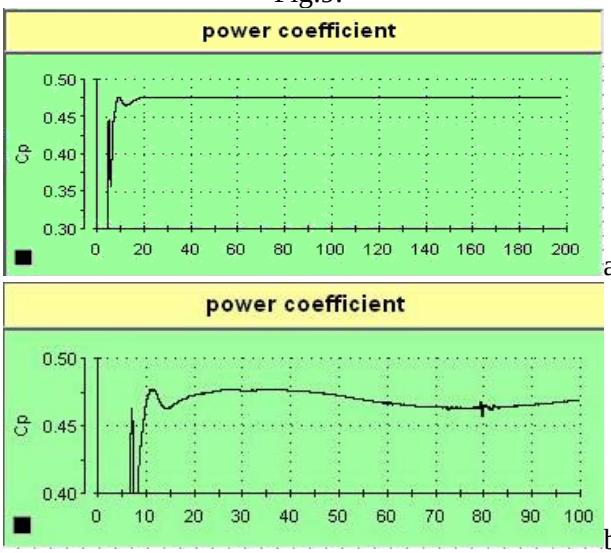

Fig.11.

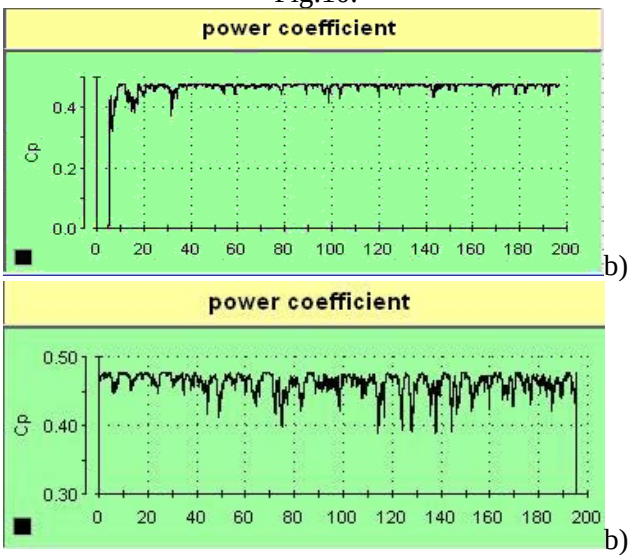

Fig.12.

The second analyzed variable is the power coefficient, $C_P(t)$. The evolution of this variable is displayed in Fig.11, first for a wind speed increasing slowly with constant gradient. For mechanical power within optimization regime the optimal power coefficient rest constant at his maximum value (Fig.11.a) since for electrical power within optimization regime it is variable (Fig.11.b). This means that the PMSG efficiency impose a wind turbine suboptimal regime for achieving the global optimal regime of the entire system.

Similar results are obtained when the wind speed varies stochastically. For mechanical power optimization regime the dynamical deviations within optimal value of the power coefficient are very smalls (Fig.12.a), since for the electrical power optimization regime are higher (Fig.12.b).

5 Conclusion

This paper has approached the problem of maximizing the global efficiency of a low-power multi-polar-PMSG-based wind energy conversion system. Two optimal regimes characteristics (ORC) can be defined: the first one represents the mechanical power versus the rotational speed (ORC_m) and the second one is the electrical power delivered to a load versus the rotational speed (ORC_e). An optimal control solution is proposed as tracking the ORC_e by means of a power loop using the measured rotational speed. The reference of this loop is computed by modelling the ORC_e as a polynomial curve. The proposed solution is validated by experimental results on a dedicated experimental rig.

References:

[1] A. Zamfir, Development of Wind Energy in European Union. 7th WSEAS International Conference on Electric Power Systems, High Voltages, Electric Machines, Venice, Italy, November 21-23, 2007.

[2] T Senjiyu, S. Tamaki, E. Muhando, N. Urasaki, H. Kijo, T. Funabashi, H. Fujita, H. Sekine, Wind velocity and rotor position sensorless maximum power point tracking control for wind generation system, *Renewable Energy*, Vol.31, 2006, pp. 1764-1775..

[3] H. Camblong, I. Martinez de Alegria, M. Rodriguez, G. Abad, Experimental evaluation of wind turbines maximum power point tracking controllers, *Energy Conversion and Management*, Vol.47, No.18-19, 2006, pp. 2846-2858.

[4] K. Tan, S. Islam, S. Optimum control strategies in energy conversion of PMSG wind turbine system without mechanical sensors, *IEEE Transactions on Energy Conversion*, Vol.19, No.2, 2004, pp. 392-399.

[5] J. Martinez, A. Morales, O. Probst, A. Llamas, C. Rodriguez, Analysis and simulation of a wind-electric battery charging system, *International Journal of Energy Research*, Vol.30, 2006, pp. 633-646

[6] J. Smajo, Rotor Power Feedback Control of Wind Turbine System with Doubly-Fed Induction Generator. Proceedings of the 6th WSEAS International Conference on Simulation, Modelling and Optimization, Lisbon, Portugal, September 22-24, 2006.

[7] J. Smajo, M. Smajo and D. Vukadinovic Reference Value Choice of the Wind Turbine Active Power with Doubly-Fed Induction Generator, 2005 WSEAS Int. Conf. on DYNAMICAL SYSTEMS and CONTROL, Venice, Italy, November 2-4, 2005 (pp379-384).

[8] K. Yukita, Y. Goto and K. Ichiyanagi Wind Generator System Using Wind Collection Equipment and Maximum Power Point Tracker System, Proc. of the 5th WSEAS/IASME Int. Conf. on Electric Power Systems, High Voltages, Electric Machines, Tenerife, Spain, December 16-18, 2005 (pp503-508).

[9] A.M. De Broe, S. Drouilhet, V. Gevorgian, A peak power tracker for small wind turbines in battery charging applications, *IEEE Transactions on Energy Conversion*, Vol.14, No.4, 1999, pp 1630-1635.

[10] B. Borowy, Z.M. Salameh, Dynamic Response of a stand-alone wind energy conversion system with battery energy storage to a wind gust, *IEEE Transactions on Energy Conversion*, Vol.12, No.1, 1997, pp. 73-78.

[11] A.S. Neris, N.A. Vovos, G.B. Giannakopoulos, A variable speed wind energy conversion scheme for connetion to weak AC systems, *IEEE Transactions on Energy Conversion*, Vol.14, No.1, 1999, pp. 122-127.

[12] I. Schiemenz, M. Stiebler, Maximum power point tracking of a wind energy system with a permanent-magnet synchronous generator, *Proceedings ICEM*, Espoo Finland, 2000, pp. 1083-1086.

[13] N.A. Cutululis, E. Ceangă, A.D. Hansen, P. Sørensen, Robust multi-model control of an autonomous wind power system, *Wind Energy*, Vol.9, No.5, 2006, pp. 399-419.

[14] Md. Arifujjaman, M. Tariq Iqbal, J.E. Quaicoe, Energy capture by a small wind-energy conversion system, *Applied Energy*, Vol.85, 2008, pp. 41-51.

[15] J. Kinnunen, *Direct-on-line axial flux permanent magnet synchronous generator static and dynamic performance*, Ph.D. Thesis, Lappeenranta University of Technology, Finland, 2007.

[16] T.F. Chan, L.-T. Yan, L.L. Lai, Permanent-magnet synchronous generator with inset rotor for autonomous power-system applications. *Generation, Transmission and Distribution, IEE Proceedings*, Vol.151, No.5, 2004, pp: 597-603.

[17] I. Munteanu, A.I. Bratcu, N.A. Cutululis, E. Ceangă, *Optimal Control of Wind Energy Systems – Towards a Global Approach*, Springer-Verlag London, 2008.

[18] C. Nichita, E. Ceangă, A. Piel, J.J. Belhache, L. Protin, Real time servo system for wind turbine simulator, *Proceedings of the 3rd International Workshop on Advanced Motion Control*, Berkely, 1994, pp. 1039-1048.

[19] C. Nichita, A.D. Diop, J.J. Belhache, B. Dakyo, L. Protin, Control structures analysis for a real time wind system simulator, *Wind Engineering*, Vol.22, No.6, 1998, pp. 275-286.

[20] A.D. Diop, C. Nichita, J.J. Belhache, B. Dakyo, E. Ceangă, Modelling variable pitch HAWT characteristics for a real time wind turbine simulator, *Wind Engineering*, Vol.23, No.4, 1999, pp. 225-243.

[21] T. Burton, D. Sharpe, N. Jenkins, E. Bossanyi, *Wind energy handbook*, John Wiley & Sons, New-York, 2001.

[22] A.D. Diop, E. Ceangă, J.L. Rétiveau, J.F. Méthot, A. Ilinca, Real-time three-dimensional wind simulation for windmill rig tests, *Renewable Energy*, Vol.32, No.13, 2007, pp. 2268-2290.

[23] C. Nichita, D. Luca, B. Dakyo, E. Ceangă, Large band simulation of the wind speed for real time wind turbine simulators, *IEEE Transactions on Energy Conversion*, Vol.17, No.4, 2002, pp. 523-529.

APPENDIX

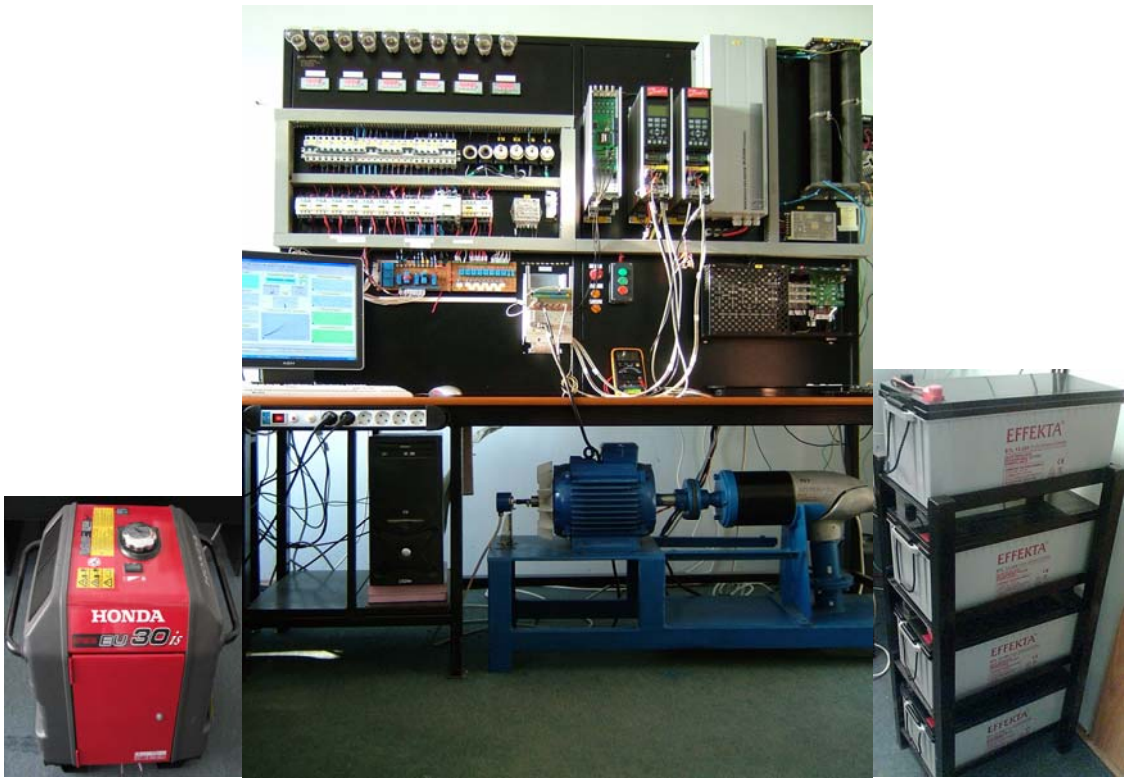

Fig.13. Picture of the experimental rig